INTERNATIONAL JOURNAL FOR NUMERICAL METHODS IN FLUIDS
Int. J. Numer. Meth. Fluids 2002; **39**:961–977 (DOI: 10.1002/fld.354)

AGE method simulations of a turbulent far-wake compared to spectral DNS

David K. Bisset*,†

Center for Turbulence Research, Bldg 500, Stanford University, CA 94305, U.S.A.

SUMMARY

Turbulent flow simulation methods based on finite differences are attractive for their simplicity, flexibility and efficiency, but not always for accuracy or stability. This paper demonstrates that a good compromise is possible with the advected grid explicit (AGE) method. Starting from the same initial field as a previous spectral DNS, AGE method simulations of a planar turbulent wake were carried out as DNS, and then at three levels of reduced resolution. The latter cases were in a sense large-eddy simulations (LES), although no specific sub-grid-scale model was used. Results for the two DNS methods, including variances and power spectra, were very similar, but the AGE simulation required much less computational effort. Small-scale information was lost in the reduced resolution runs, but large-scale mean and instantaneous properties were reproduced quite well, with further large reductions in computational effort. Quality of results becomes more sensitive to the value chosen for one of the AGE method parameters as resolution is reduced, from which it is inferred that the numerical stability procedure controlled by the parameter is acting in part as a sub-grid-scale model. Copyright © 2002 John Wiley & Sons, Ltd.

KEY WORDS: turbulent shear flow; planar wake; finite difference; DNS; LES; advected grid

1. INTRODUCTION

The advected grid explicit (AGE) method has proven to be both efficient and accurate for simulating turbulent free-shear flows, including planar mixing layers and planar jets. There are two main reasons for its efficiency. First, the localized fully explicit finite difference formulation [1, 2] is very straightforward to compute, which outweighs the need for a fairly small timestep. Second, most of the successful simulations were slightly under-resolved, and therefore they were, in effect, large-eddy simulations (LES) without a sub-grid-scale (SGS) model, rather than direct numerical simulations (DNS). The principle is that the role of the smallest scales of turbulent motion (when the Reynolds number is not too low) is to dissipate turbulent energy, and therefore they do not have to be simulated when the numerical method is inherently dissipative at its resolution limits. This idea has been called ‘pseudo-direct

*Correspondence to: D. K. Bisset, 103 Nemarang Crescent, Waramanga, ACT 2611, Australia.
†E-mail: bissli@ozemail.com.au

Received February 2001
Revised December 2001

simulation' [3], but a name related to LES seems preferable given that not all scales are resolved, so the term 'auto-LES' (LES with automatic SGS modelling) will be used in this paper. It is demonstrated in Section 6 that certain aspects of the AGE method designed for numerical accuracy and stability also behave somewhat like a Smagorinsky-type SGS model.

A brief summary of the main features of the AGE method, as generally implemented [1, 2], is as follows. First, the AGE method is based on the incompressible Navier–Stokes equations (velocity/pressure formulation), except that the density is not assumed to be exactly constant. Consequently an equation for pressure fluctuations is derived from mass continuity and an equation of state. Pressure values are somewhat smoothed as they are updated, controlled by parameter W_P. See Section 6.4 for discussion of some aspects of the pressure calculations. Second, the grid is advected through the calculation domain during spatial simulations of flows with large mean velocities. On the advecting grid the magnitudes of large non-linear terms are reduced. Third, the growth of certain numerical instabilities is prevented by 'targeted diffusion', controlled by parameter W_V; see Section 6.2. Fourth, time advancement is entirely explicit; it is first-order forward in the present case. Timestep size limitations are reduced by the selection of an appropriate sonic speed for the fluid. Fifth, spatial derivatives are centred finite differences, second order in the present case, but defined in a special way that accounts for local fluid advection relative to the grid ('dynamic derivative offset', see Section 6.3).

The quality of a numerical method must be judged ultimately through comparisons with experimental results, but there is always the difficulty of not knowing the exact initial or boundary conditions in turbulent flow experiments. This problem can largely be overcome when comparing with other numerical simulations (although the question of which simulation is correct might then arise if they disagreed). The aims of this work are (a) to compare, in terms of accuracy and efficiency, a well-resolved AGE method DNS with a high-quality spectral DNS under identical conditions, and (b) to assess the effects of reducing the resolution, that is to compare AGE method auto-LES of the same flow with the DNS results. In both cases the effects of the two adjustable parameters in the AGE method are to be determined.

The comparison spectral DNS is a temporally evolving plane wake of a parallel flat plate with turbulent boundary layers simulated by Moser *et al.* [4], using the method of Spalart *et al.* [5]. This flow has also been simulated with spectral LES by Ghosal and Rogers [6] from almost identical initial conditions. The flow is very similar (including Reynolds number) to some of the experiments carried out by Weygandt and Mehta [7], but the simulations use a particular realization of turbulent boundary layers for their initial state, and only results from an ensemble of many different initial realizations should be expected to agree fully with experimental statistics. A real wake develops spatially rather than temporally, but the temporal approximation to spatial development is very good in a far-wake (the streamwise rate of change of properties is very slow) and is not likely to cause differences. The streamwise-periodic boundary conditions used in temporal simulations simplify the problem very significantly and also match exactly the assumption of periodicity inherent in spectral methods.

Previous AGE results have all come from flows developing spatially with inflow and outflow boundary conditions. Two-stream mixing layers [1, 2] may develop quite rapidly, depending on velocity ratio, and a turbulent jet into still surroundings [8] develops very rapidly through several distinct stages. With realistic inflow conditions, the correct asymmetrical mixing of a scalar in a two-stream mixing layer was obtained [9]. The present comparison using periodic boundary conditions is therefore not a complete test of the AGE method as usually applied. In fact the 'advected grid' feature is not being used at all in the numerical sense, because the

mean flow of the wake has been removed from the problem by the temporal transformation, and the original fixed physical boundaries are irrelevant after the computations begin. Thus, a temporal flow comparison results in a slightly less demanding test of AGE capabilities, but this is outweighed by the opportunity to compare with another method under well-defined conditions. On the other hand, the efficiency advantage of the AGE method is less significant in temporal simulations than in spatial, because adequate statistics can be obtained from one or a few realizations of a temporal simulation averaged in the streamwise and spanwise directions, while spatial simulations are more like experiments with probes sampling at fixed positions, and must be run until statistics (possibly spanwise-averaged) converge.

Given the philosophy behind the development of the AGE method [1] that somewhat favours efficiency in the trade-offs between efficiency and accuracy, the results to follow show a very satisfactory level of agreement. Further, this agreement is in contrast to the quite different results that were obtained from another AGE simulation with different initial conditions, discussed briefly at the end of the next section. Parts of this work have also been discussed in Reference [10].

2. CONDITIONS FOR DNS

Moser *et al*. [4] numerically simulated the wake of a parallel flat plate with turbulent boundary layers at a Reynolds number $\dot{m}/\nu = 2000$, where $\dot{m}$ is the cross-stream integrated mass flux deficit per unit depth spanwise normalized by density, or in other words, the mean velocity deficit $\langle U \rangle$ integrated over y. Angle brackets indicate averaging over any plane of constant y, the temporal equivalent of a spatial or experimental time average at a point, which is denoted by an overbar. Lower case letters indicate fluctuations, thus $U = \langle U \rangle + u$. The initial state was obtained by placing data from two different instants in Spalart's [11] boundary layer simulation back-to-back (without the wall) in a periodic domain of size $50\dot{m}/U_\mathrm{d}$ streamwise and $12.5\dot{m}/U_\mathrm{d}$ spanwise, where U_d is the mean centreplane velocity deficit initially. The simulation was carried out for 125 time units $\tau = tU_\mathrm{d}^2/\dot{m}$ with a variable timestep Galerkin incompressible spectral method [5] using up to $512 \times 195 \times 128$ modes (adjusted several times during the total run). From $\tau = 40$ the mean velocity profile was self-similar when normalized by the centreplane velocity defect U_0 and the half-velocity width b, and the growth rate $(1/U_0)\,\mathrm{d}b/\mathrm{d}t$ was constant, but by $\tau = 100$ the spanwise correlation length was becoming too large for the domain, and self-similarity broke down. Results will be shown near the beginning ($\tau = 42.8$) and especially near the end ($\tau = 91.5$) of this range. Note that b is taken from the full $\langle U \rangle$ profile, not the half profile as used by some authors.

For the AGE simulation, spectral vorticity data from $\tau = 1.4$ were converted to velocity components on a $514 \times 320 \times 130$ physical grid with $\Delta x = \Delta z = 1.95\Delta y$, and 10-point-thick damping layers at the top and the bottom. The AGE method does not assume precisely incompressible flow, and therefore an initial pressure field was calculated separately with a Poisson equation. The velocity of pressure waves (acoustic velocity c) should be kept reasonably low, because the timestep size limit is inversely proportional. It was adjusted so that U_0 was about $0.3c$ initially; U_0 decreased through the run to finish at less than $0.08c$, which means that the flow was effectively incompressible in terms of usual laboratory practice. The timestep was set to $\Delta\tau = 0.02$, the acoustic maximum based on Δy. Parameters W_P (pressure smoothing) and W_V (targeted diffusion) were varied, as detailed later. The same

grid was used for the whole run, but at $\tau = 91.5$ the irrotational fluctuations in the free stream were beginning to impinge on the upper and lower damping layers, and it would have been advisable to enlarge the domain in y for any further calculations.

Both spectral and AGE calculations included a passive scalar, but a first-order upwind method was used for the scalar in the AGE calculations, and it was not expected that the results for the scalar would compare as well as the velocity results. In fact the distribution of the mean scalar value was quite reasonable in the DNS, but scalar variances were somewhat lower (more so in the auto-LES cases) than the spectral DNS values because of excessive numerical diffusion. The impact of the pressure calculation on the advection of momentum (by contrast with advection of the scalar) is discussed later. Future AGE simulations will use an improved scalar advection scheme, so the present results will not be considered further.

Another temporal wake was simulated as a preliminary test, mainly to 'calibrate' the scale of any differences between AGE and spectral results in the main comparison. The spectral simulation results for Reynolds stresses, for example, were significantly lower than those of quite a number of self-similar far-wakes, and it was not clear in advance how well the AGE method simulation would respond to the strong boundary layer effects in the initial velocity field.

The preliminary simulation began from a simple top-hat velocity profile with a small amount of random noise superimposed along the planes of the velocity discontinuity, rather like the wake of a screen or porous plate normal to the flow. A much larger spanwise domain was used so that the calculation continued to $\tau = 140$ without reaching the spanwise correlation limit. The mean velocity profile was approximately self-similar from $\tau = 10$ onwards. Self-similarity was achieved sooner in this case at least in part because of the normalization with U_d (no cusp in the mean velocity profile in this wake). In contrast to the main simulation results, the normalized Reynolds stress profiles were larger in the early stages (after the initial rollup and interaction of the two mixing layers) and decreased slowly during the rest of the calculation. This behaviour is typical of most far-wakes including wakes of parallel plates with *laminar* boundary layers [7]. The rate of change of the profiles was slow enough that they could be considered self-similar over much of the period, and they were much closer to the experimental results (Reference [7], or Figure 5 of Reference [4]) than were the main simulation results. Most importantly in the present context, the differences between the top-hat wake and the wake from turbulent boundary layers turned out to be vastly greater than the differences between the AGE and spectral versions of the latter.

All of the AGE DNS runs were carried out on the Fujitsu VPP300 at the Australian National University Supercomputer Centre. The spectral DNS and AGE auto-LES were performed on a Cray C90 at NASA Ames Research Center.

3. CONDITIONS FOR AUTO-LES

The starting fields for the auto-LES runs were obtained by simply omitting data points (one out of two, two out of three, or seven out of eight, in each direction) from an instant in the AGE DNS calculation. The reduced grids are denoted R2, R3 and R8 respectively. At $\tau = 1.4$, the original starting point, the cusp in the mean velocity profile was too sharp to be represented accurately in the reduced data, so the instant $\tau = 10.4$ was chosen. Here the mean velocity profile is still far from its self-similar form, but the peak value has dropped

by more than 50% and the cusp has begun to spread out. Several W_P and W_V values were used as detailed later. The timestep was increased to the acoustic limit for each level of data reduction. Upper and lower damping layers were maintained at 10 points thick, so the R8 grid was $66 \times 58 \times 18$ points. More than 99.8% of the original undamped data points were eliminated in this case.

No changes were made to the AGE method algorithm, and in particular there was no SGS model, but it will be shown later that the 'targeted diffusion' routine controlled by parameter W_V may be acting a bit like a SGS model even though its primary purpose is numerical stability, and the definition of derivatives used in non-linear terms may also produce that effect.

4. AGE DNS RESULTS

Growth of the wake width b and decay of the centreplane velocity defect U_0 are shown in Figure 1, arranged such that they would be linear functions of time for self-similar velocity profiles. AGE parameter values for all DNS results in this section were $W_V = 1.5$ and $W_P = 0.5$, but the parameter values for DNS are not at all critical as shown in Section 6. Halfwidth values from the AGE DNS agree quite well with spectral results, but U_0 is tending to decay slightly more quickly, and at $\tau = 91.5$ it is low by about 3%. Normalized mean velocity distributions (not shown) from $\tau = 40$ onwards collapse very well onto the spectral self-similar results (see Figure 3(a) of Reference [4] for the latter). While the slightly faster decay of U_0 is undesirable, it should be viewed from the perspective that the growth rates (in b) of most far-wakes are of order 50% larger, as discussed in Reference [4], and therefore the AGE simulation has retained virtually all of the effects of the turbulent boundary layer initial conditions in this case.

The effects of the two different boundary layer realizations on the two sides of the wake are actually somewhat different, which appears most clearly in profiles of $\langle v^2 \rangle$, the variance of the transverse velocity fluctuations, shown in Figure 2. Compared to free shear flows, boundary layers tend to have relatively less energy in the transverse and spanwise fluctuations, and shorter spanwise length scales, so it is not surprising that $\langle v^2 \rangle$ increases during the earlier

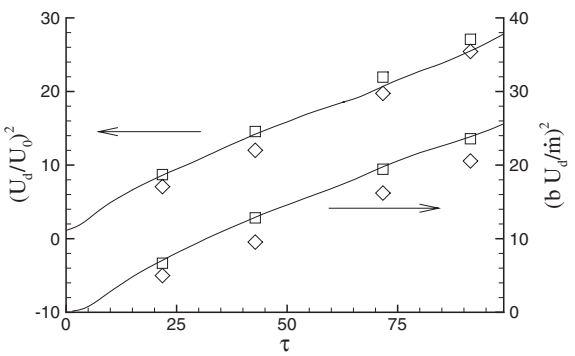

Figure 1. Decay of centreplane mean velocity U_0 and growth of wake halfwidth b for spectral DNS (lines), AGE DNS (squares) and auto-LES on grid R8 (diamonds).

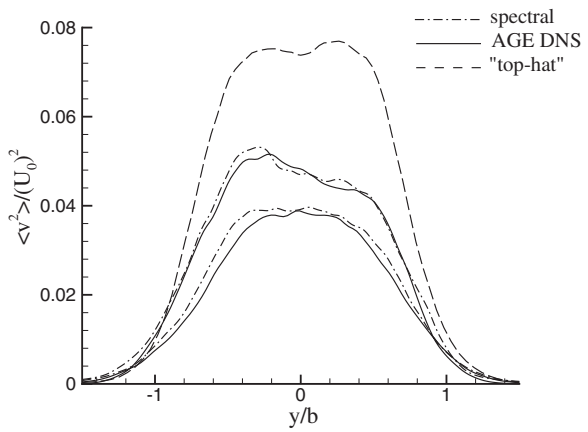

Figure 2. Distributions of $\langle v^2 \rangle$ from spectral and AGE DNS at $\tau = 42.8$ (lowest curves) and $\tau = 91.5$ (middle curves). The uppermost curve is $\langle v^2 \rangle$ at $\tau = 74.4$ from the top-hat initial profile.

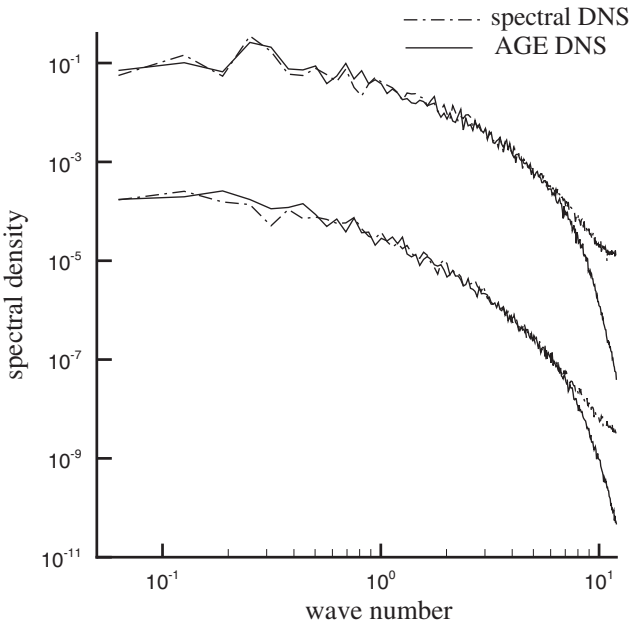

Figure 3. Streamwise power spectra of u (lower curves) and v (upper curves) from AGE DNS and spectral DNS at $\tau = 91.5$ on the centreplane.

stages of this simulation, nor that the spanwise correlation length becomes the limiting factor in a domain where the width originally suited a boundary layer. The continuing slow increase in $\langle v^2 \rangle$ throughout the self-similar period (Figure 2), in contrast to profiles of other quantities, is analysed in Reference [4]. The increase in $\langle v^2 \rangle$ is a little faster on the lower side of the

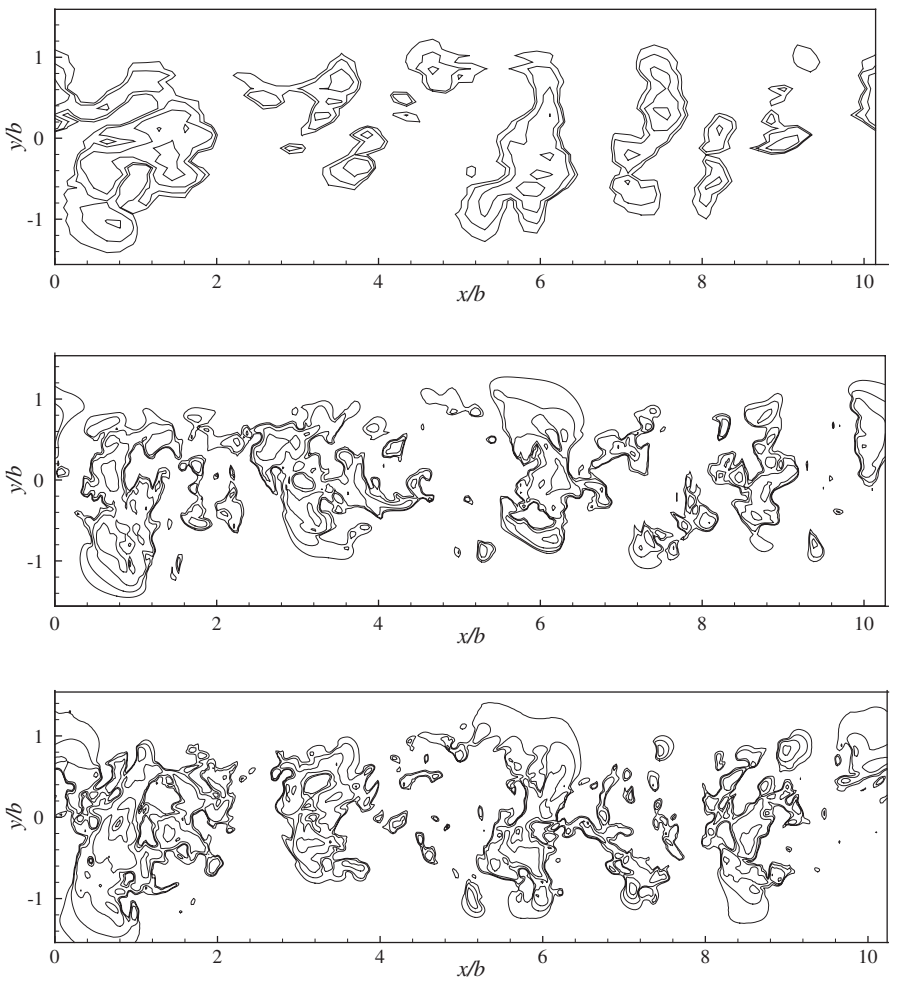

Figure 4. Positive contours of transverse velocity V at $\tau = 91.5$, $z/b = 0$, from the spectral DNS (bottom), AGE DNS (middle) and auto-LES on grid R8 (top). Contours $V/U_0 \approx 0.05, 0.1, 0.2, 0.4$.

wake, giving a rather asymmetrical profile at the later time in Figure 2. Clearly the results for the two simulation methods are very similar. Agreement for other profiles (not shown) such as $\langle uv \rangle$ is equally good, except that the spectral DNS $\langle u^2 \rangle$ profile is more asymmetrical than the AGE version at the final time. The close agreement in Figure 2 for the same initial conditions may be contrasted with the results obtained from other initial conditions, i.e. the top-hat profile, also shown in Figure 2 at an intermediate time.

The same trend of growth in $\overline{v^2}$ profiles from the early stages of wakes of parallel plates with turbulent boundary layers can be seen in the experiments of Weygandt and Mehta [7] (Figure 21c), and there is a rough correspondence between profile peak values in the experiments and DNS for similar values of U_0/U_d. Wakes after laminar boundary layers have $\overline{v^2}$ profiles that are much stronger initially and slowly decrease [7].

Figure 3 compares streamwise power spectra of the fluctuations u and v from the centreplane at $\tau = 91.5$ from both DNS methods. Except at very high wavenumbers, the agreement is remarkably good, and where they begin to diverge the levels of the spectra have already decreased by three to four orders of magnitude. Most likely the modified second-order central differencing used with AGE is too diffusive at very small scales (high wavenumbers), but it is also likely that some residual noise has raised the spectral DNS values slightly at high wavenumbers, especially for the v spectrum.

The comparative results so far have involved progressively less averaging, from global through to spectral properties, but the next comparison—instantaneous contours of a velocity component—involves no averaging at all. At this level the effects of initial or early-time deviations that have been magnified through thousands of subsequent timesteps are likely to be noticeable, even though statistical properties were not affected.

Contours of positive values of V are shown in Figure 4. The general placement of V contours, corresponding to the large scales of turbulent motion, shows good agreement, but the detailed level of agreement at smaller scales is rather variable. Roughly the same sizes and numbers of concentrated high-value contours of V can be found, however, which leads to statistical similarity. Results for the other velocity components and results in (x,z) planes show a similar level of agreement between the two DNS methods.

CPU time for the spectral DNS to reach $\tau = 91.5$ was around 180 Cray C90 hours. The AGE DNS required 5.0 h on a Fujitsu VPP300, which corresponds to about 11.5 h on the Cray, based on a direct comparison of a similar code run identically on the two machines. The AGE computer code is also significantly shorter and simpler to write than the spectral code.

5. RESULTS FOR AUTO-LES

The growth of b and decay of U_0 for grid R8 have already been shown in Figure 1. Considering that at $\tau = 10.4$ (when the projection onto R8 was made) more than 50% of the change in mean velocity across the wake occurs within two grid points either side of the centreplane, the effect of reducing the data to R8 is quite small, especially for U_0. Also, the rate of change of b is about right even though values of b are a bit low (a consequence of poor representation of the velocity defect initially). Results on R2 and R3 were closer to the DNS. The value $W_V = 2.2$ for the targeted diffusion parameter was used here for grid R8, as it produced the best results for power spectra (see below). Reducing W_V decreased the magnitude of U_0 and increased b, and vice versa for larger W_V. The value of the parameter W_V has a significantly greater effect on auto-LES results than on DNS, as described in Section 6.

The effect of reduced resolution on $\langle v^2 \rangle$ is shown at $\tau = 91.5$ in Figure 5, using $W_V = 1.5$ for all except R8. The curve for the R2 case deviates a little from the DNS, and for R3 the values are slightly large on the upper side of the wake. For R8, the distribution is somewhat narrower overall, even though b, the normalizing factor, is smallest for R8. Roughly the same level of agreement was found for other variances and for Reynolds shear stress (not shown). Clearly the reduction in resolution with auto-LES is not degrading the results in any serious way, and the missing small scales do not contribute a great deal to the total turbulent energy.

Power spectra for velocity components u and v are presented in Figure 6, along with the corresponding pressure spectra. At the high wavenumber end, reduced resolution causes a

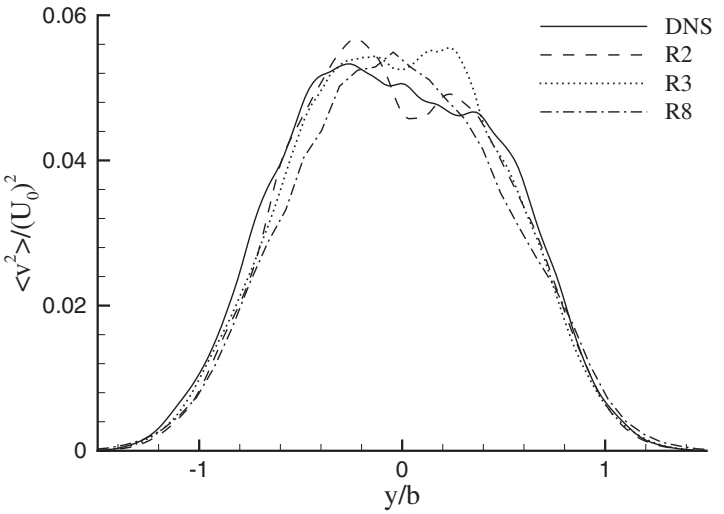

Figure 5. Distributions of transverse velocity variance at $\tau = 91.5$ for AGE DNS and for auto-LES at three levels of resolution.

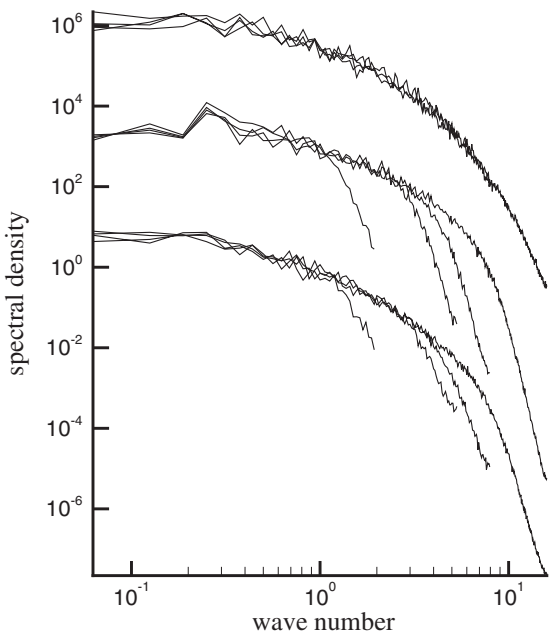

Figure 6. Power spectra on the centreplane at $\tau = 91.5$ for u (bottom), v (middle) and pressure (top) from AGE DNS and auto-LES. From left to right by rolloff point, the grids used were R8, R3, R2 and DNS.

progressively earlier rolloff in the spectra, but values before the rolloff points are remarkably consistent. As mentioned above, W_V was increased to 2.2 for grid R8 in order to match the spectra (values were somewhat high at $W_V = 1.5$), but no other changes were made. Interestingly the pressure spectra do not exhibit any rolloff, although the overall level on R8 is affected by W_V just as for velocities. This and other aspects of the pressure calculation will be discussed further in the next section.

Contours of V on the R8 grid have already been shown in Figure 4(c), and they imply quite reasonable similarity between large-scale motion in the auto-LES and DNS. In contrast, small scale concentrations of V are rarely seen on the coarse grid. After a longer calculation time in a larger domain, an auto-LES would probably differ significantly from DNS on an instantaneous basis even at larger scales, but it is reasonable to expect that the current level of agreement would be maintained for statistical averages.

CPU times on the Cray C90 for the three levels of auto-LES, scaled to include the missing time before the transfer from the DNS grid at $\tau = 10.4$, were 52 min (grid R2), 13 min (R3), and less than 40 s (R8). The ideal speedup goes as the fourth power of grid spacing (the timestep is enlarged along with the grid), but vector overheads and the fixed thickness damping layers reduce the actual speedup somewhat. CPU time for the LES by Ghosal and Rogers [6] with a dynamic SGS model was an order of magnitude greater at resolution similar to R8.

6. SOME NUMERICAL ASPECTS OF THE AGE METHOD

6.1. Parameter values for DNS and auto-LES

Selected values of the AGE parameters W_V and W_P were used for the results presented above, but now the effects of changing those values will be considered in the contexts of DNS and auto-LES.

The pressure smoothing parameter W_P (see Reference [1]) can be dealt with very quickly: over the range of at least $0.2 \leqslant W_P \leqslant 0.9$, the value of W_P has very little effect on both DNS and auto-LES results, including pressure variances and power spectra as well as velocity results. At $W_P = 0.99$ (almost no smoothing) on the R8 grid, however, a large amount of numerical noise had built up by the end of the run, and the simulation was starting to break down. Although no similar run was tried at DNS resolution, previous experience with mixing layers and jets suggests that the same problem would occur for an AGE DNS of a wake given a long enough calculation time. In summary, pressure smoothing does play a crucial role for AGE calculations, but its controlling parameter value is not at all critical within quite a large range.

The setting of the targeted diffusion parameter W_V [1] was expected to have a greater influence on results. For example, auto-LES of a fairly high Reynolds number spatially developing mixing layer showed some effect from the W_V value even though the resolution was approaching DNS [2]. However, the wake DNS (for which W_V was set to 1.5 initially) was repeated with $W_V = 1.0$ and $W_V = 2.5$ with remarkably little change in the results. Transverse variances are presented in Figure 7, where a very slight increase is seen for $W_V = 2.5$; there is no significant difference in V power spectra (Figure 8). Targeted diffusion was originally derived with $W_V = 1.0$ [1], but higher values were needed in practice. Present experience seems to support

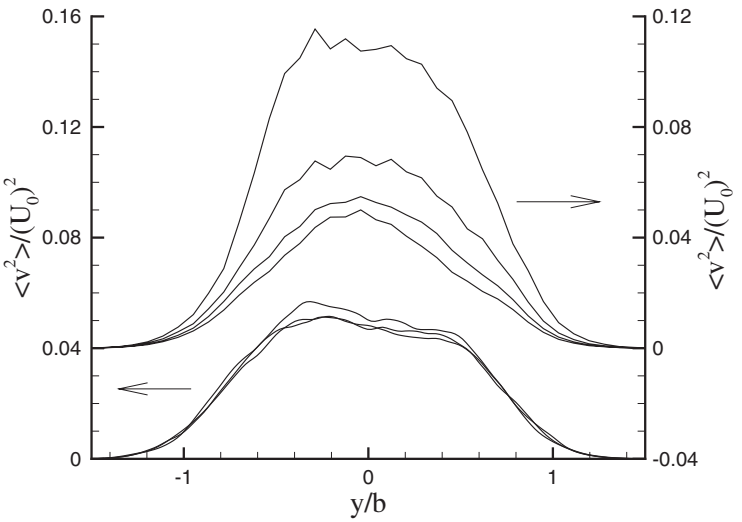

Figure 7. Effect of targeted diffusion parameter W_V on $\langle v^2 \rangle$ at $\tau = 91.5$. For DNS (lower group) the W_V values from bottom to top were 1.0, 1.5 and 2.5; for auto-LES on grid R8 (upper group), 3.0, 2.2, 1.5 and 1.0 (bottom to top).

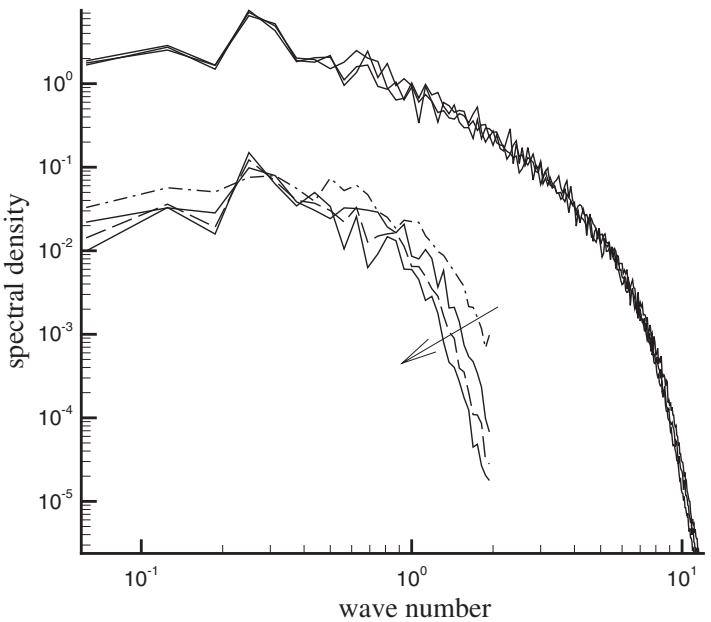

Figure 8. Effect of targeted diffusion parameter W_V on transverse velocity spectra at $\tau = 91.5$. W_V values as in Figure 7. For auto-LES on grid R8 (lower curves) W_V increases as shown.

the original concept for DNS. Further runs were attempted with $W_V = 0$ (i.e. targeted diffusion switched off completely) or $W_V = 0.5$, but the calculations were unstable and eventually broke down, showing that targeted diffusion does play an important role, even in a DNS.

The setting of W_V has much more influence on auto-LES results, especially when the coarse R8 grid is used. As shown in Figure 7, $\langle v^2 \rangle$ more than doubles when W_V is decreased from 2.2 (the selected value initially) to 1.0, and for $W_V = 3.0$, $\langle v^2 \rangle$ decreases slightly. Power spectra are also affected significantly (Figure 8). A problem for auto-LES in other flows then arises: is it possible to set W_V correctly without having to do the corresponding DNS? All that can be said with certainty at this stage is that a test of sensitivity to the W_V value should be carried out, and the best W_V is somewhat larger than 1.0 if the results are affected. In future it may be possible to set W_V as a function of a grid Reynolds number.

6.2. *A grid Reynolds number for targeted diffusion*

The idea behind targeted diffusion is that the current value of a velocity component in a time advancement equation should always be multiplied by a coefficient in the range 0.0–1.0, with the upper limit being the important case for turbulent flow [1]. When the coefficient would go above 1.0 the particular velocity component is modified in a manner that amounts to a temporary local increase in diffusion, at a level controlled by W_V.

In the equation for finding the new value of U, the coefficient of the current U value is

$$\left[1.0 - \frac{\Delta t}{2\Delta x}\Delta U - \Delta t \nu \left(\frac{2}{(\Delta x)^2} + \frac{2}{(\Delta y)^2} + \frac{2}{(\Delta z)^2}\right)\right]$$

which can be greater than 1.0 if ΔU (the velocity difference across $2\Delta x$) is negative. For simplicity let $\Delta x = \Delta y = \Delta z$, and then set the coefficient equal to 1.0:

$$1.0 - \frac{\Delta t}{2\Delta x}\Delta U - \Delta t \nu \frac{6}{(\Delta x)^2} = 1.0$$

which reduces to

$$Re_G = \frac{(-\Delta U)\Delta x}{\nu} = 12$$

Therefore, the problem yields a grid Reynolds number Re_G, and the coefficient of the current U value exceeds 1.0 when $Re_G > 12$. The critical value varies when grid spacing is different in different directions—in this work it is 23, because $1.0/\Delta y = 1.95/\Delta x$.

On the R2 grid, in the fully turbulent zones, $Re_G > 23$ on about 3.3% of the occasions for which $\Delta U < 0$, but the proportion on R8 is 77%. Re_G values have not been determined for the DNS, but Δx is smaller and ΔU is correspondingly smaller when calculated over that spacing, so Re_G is nearly quadratic in Δx. Therefore, it is likely that the critical value of Re_G is only rarely exceeded in the DNS, at least in the later part of the simulation. It seems that targeted diffusion is controlling these occasional overshoots in the DNS (the calculation eventually becomes unstable if targeted diffusion is switched off), but otherwise it is having little effect in comparison with the true diffusion terms. On the other hand, it was shown that although the 'ideal' value $W_V = 1.0$ is usually sufficient for stability on auto-LES grids, higher values are needed for quality results. Here it is possible that the targeted diffusion term is acting as a SGS model, increasing diffusion locally when there is a high local deceleration in

the direction of flow (large negative ΔU). [One might note that strong local *accelerations* also need SGS diffusion (vortex stretching, etc.), but this will occur, when appropriate, through decelerations induced in other velocity components.] Cross-stream gradients do not appear in the targeted diffusion calculations, so there is no effect similar to the problems sometimes found with standard SGS models in pre-transition regions with high laminar shear.

It is hoped that it will eventually be possible to set the correct value of W_V in reduced-resolution AGE simulations by relating W_V to the Re_G values, but more experience is needed.

6.3. Analysis of DDO

The present version of the AGE method [2] utilizes in the non-linear terms a particular form of velocity derivative invoking 'dynamic derivative offset' (DDO), and it has been pointed out by B.J. Boersma (private communication) that the offset terms have the same general form as the Smagorinsky-type SGS model frequently used for LES. The suggested analogy is described below and then discussed.

Denoting the calculated large-eddy quantities in a standard LES by $(\tilde{.})$, and considering for simplicity just one non-linear term $\tilde{U}\partial\tilde{V}/\partial x$ in the time advancement equation for $\tilde{V}$,

$$\tilde{U}\frac{\partial\tilde{V}}{\partial x}=\frac{\partial}{\partial x}(\tilde{U}\tilde{V})+\frac{\partial}{\partial x}(\widetilde{UV}-\tilde{U}\tilde{V})-\tilde{V}\frac{\partial\tilde{U}}{\partial x}$$

The last term on the right-hand side disappears through continuity for incompressible flow (the full equation includes $\tilde{V}\partial\tilde{V}/\partial y$ and $\tilde{V}\partial\tilde{W}/\partial z$), the first term is calculated, and the middle term is modelled as the gradient of a SGS stress τ; thus

$$\tilde{U}\frac{\partial\tilde{V}}{\partial x}=\frac{\partial}{\partial x}(\tilde{U}\tilde{V})+\frac{\partial\tau}{\partial x}$$

The Smagorinsky model is the basis for the most commonly used model for SGS stress [12, 13], in which $\tau=-2(C_S\Delta)^2|\tilde{S}|\tilde{S}$, where C_S is a flow-dependent constant, Δ is a filter width usually related to grid spacing, and $\tilde{S}=\frac{1}{2}(\partial\tilde{U}_i/\partial x_j+\partial\tilde{U}_j/\partial x_i)$ is strain rate. The terms can be regrouped to obtain $-2C_S^2\times\Delta\times(\Delta|\tilde{S}|)\times\tilde{S}$, essentially the product of a length, a velocity, and velocity gradients.

In the AGE method, the DDO version [2] of the equivalent term is

$$U\frac{\partial V}{\partial x}=U_G\left.\frac{\partial V}{\partial x}\right|_G-\frac{U_G\Delta t}{2}U_G\left.\frac{\partial^2 V}{\partial x^2}\right|_G$$

where subscript G implies that a quantity is evaluated in the normal manner at the current grid position. The group on the right is a correction arising from the consideration that the best place to evaluate $\partial V/\partial x$ is actually upstream from the current grid position by an advection-dependent offset $L=(U_G\Delta t/2)$; see Reference [2] for further information. The correction term can be rewritten as

$$-\frac{U_G\Delta t}{2}U_G\left.\frac{\partial^2 V}{\partial x^2}\right|_G=-LU_G\frac{\partial}{\partial x}\left(\frac{\partial V}{\partial x}\right)=\frac{\partial}{\partial x}\left(-LU_G\frac{\partial V}{\partial x}\right)$$

since L and U_G are constants locally.

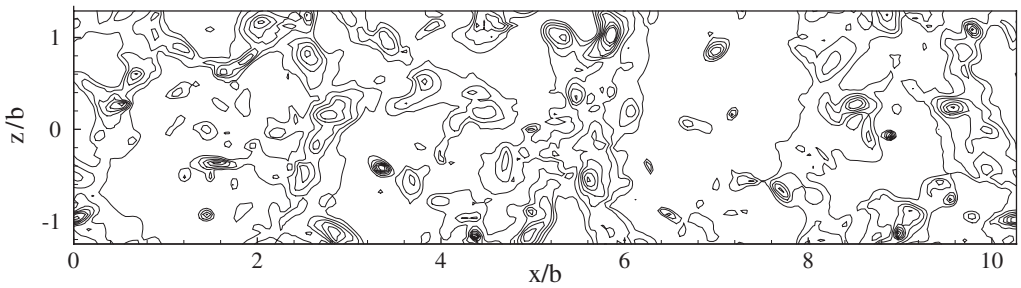

Figure 9. Contours of pressure relative to ambient from the AGE DNS at $\tau = 91.5$ in the plane $y = 0.4b$; contours $\Delta P/(0.5\rho U_0^2) = -0.1, -0.2, -0.3 \ldots$.

The quantity in the last set of parentheses has the same form as the SGS stress when the latter is regrouped as shown above, i.e. length × velocity × velocity gradient. The AGE Δt is usually scaled with Δx, so the length L tends to scale the same way as the LES Δ. The velocity gradient $\partial V/\partial x$ (AGE) is one component of $\tilde{S}$ (LES), which leads to further similarity. The analogy is not good for the velocity itself, however, since the AGE U_G is not closely related to the LES $\Delta|\tilde{S}|$, and U_G also depends on the grid advection velocity. Nevertheless, the analogy between AGE and LES under present conditions is reasonable because the factors that affect U_G were held constant while grid resolution was reduced, and thus the effect of DDO correction increased roughly in proportion to the need for a SGS contribution (along with the effects of targeted diffusion discussed in Section 6.2). For the general case, DDO was derived from physical considerations based on advection, and therefore it is reasonable that its effect depends (via U_G) on factors not related to SGS stress.

Ferziger [13] points out that although there are various objections to Smagorinsky-type models for LES, they may work well in practice because the modelled small scales are often quite similar in different flows and do not contribute very much to turbulent energy, transport properties, and so on. The main differences between flows are found in the large scales, which must be computed correctly by the LES code. Likewise, the AGE method procedures that have the effects of SGS stress may contribute to the robust behaviour of the AGE method at reduced resolution without necessarily being ideal SGS models. Other researchers, e.g. Boris *et al.* [14], have made similar suggestions about other CFD methods. Numerical diffusion can be more important than the SGS model in LES methods for transonic flow, e.g. Garnier *et al.* [15].

6.4. Aspects of the pressure calculation

The AGE method is a little unusual amongst DNS methods for incompressible flow in its use of pressure as a fundamental calculation variable, so it is worth considering a few aspects of the pressure calculation and its results. An example of low-pressure zones, which generally correspond to the cores of rotational structures, is given in Figure 9.

Firstly, it has already been noted that pressure spectra do not show the same rolloff as velocity spectra on the auto-LES grids (Figure 6). The reason for this is at least partly that

the pressure evolution equation

$$\frac{\partial P}{\partial t} = -c^2 \rho \left(\frac{\partial U}{\partial x} + \frac{\partial V}{\partial y} + \frac{\partial W}{\partial z} \right)$$

has no advection terms, unlike the velocity equations, and therefore it is not subjected to the small-scale diffusion and dispersion that often afflict advection in finite difference methods. Also, for incompressible flow the sum of the three velocity gradients involved in pressure evolution is usually much less than the magnitudes of the individual gradients; numerical diffusion tends to smooth out small-scale velocity gradients, but it will not necessarily reduce them equally at every point, and therefore their sum could be either larger or smaller than the true value.

This explanation is supported by another phenomenon, that is, any disturbance to the velocity field can produce surprisingly large short-lived excursions in the pressure field. For example, the initial velocity field and its corresponding pressures calculated from a Poisson equation (assuming pure incompressibility) do not comprise an exactly consistent state for AGE DNS. As a result, the rms of pressure fluctuations increased by around 50% within the first four timesteps, but then settled down very quickly (20 or so steps) to a stable level. Velocity variances were essentially unchanged, however, as should be the case over such a short time. Similarly, the transfer from AGE DNS to the R2 grid caused an alarming 100% increase in rms pressure after four timesteps (even higher for R3 and R8), but again the excess values disappeared quickly and other quantities were unaffected. Clearly the adjustments made to the velocity components (through temporary increases in pressure gradients for a few timesteps) were very small and rapidly achieved, but the balance in the pressure calculation was disturbed quite significantly while the adjustments were made.

Pressure plays another role in the numerical aspects of the AGE method, namely, it controls overshoot in the velocity advection terms. Second-order central differences (as used in the present calculations) are subject to the Gibbs phenomenon, which often results in overshoot of transported values of any quantity. In fact it has been necessary to avoid second-order central differences for advection of the passive scalar in order to prevent overshoot of its values. However, the scalar is not connected to the pressure calculation, whereas any tendency for a velocity component to overshoot immediately causes a counteracting pressure gradient, and therefore velocity overshoot is controlled.

At this point it is reasonable to ask whether the numerical role of pressure interferes with its true status as a physical quantity. Firstly, the correct physical formulations are used (AGE is only superficially related to artificial compressibility methods, for example, that use pressure as a purely numerical device). Secondly, two recent results support pressure's physical status in AGE. Antonia *et al.* [16] analysed pressure structure functions for 11 simulations from various sources, including two AGE spatial simulations. They found that all structure function distributions have a similar shape, and that there was a consistent trend with microscale Reynolds number. Also, preliminary results from an AGE DNS of turbulent channel flow driven entirely by the overall pressure drop show a very good balance between mean pressure gradient and wall shear stress. These results indicate that the pressure calculation is likely to be physically realistic in terms of both large-scale behaviour (e.g. mean pressure gradients) and local properties (e.g. structure functions). The one aspect that has not been tested systematically is the effect of compressibility: how far can sonic speed be lowered (and the timestep correspondingly enlarged) without affecting the results. This knowledge will be

important for wall-bounded flows where the grid spacing is usually small close to the wall, severely limiting the timestep.

7. DISCUSSION AND CONCLUSIONS

An important issue for a comparison of the present type is the extent to which it can be expected that two different simulation methods should agree. As noted earlier, close agreement between statistics from one temporal realization and converged statistics from an experiment cannot always be expected, but the present work compares two temporal simulations that begin from nominally the same initial state. However, the well-known 'butterfly effect' [17] is applicable in such a case—the idea that small uncertainties in the initial state of a turbulent flow can grow rapidly (on the timescale of the small-scale motions) and quite soon influence the evolution of even the largest scales. [Lorenz [17] actually discusses the possible magnitude and timing of changes in the earth's weather caused by one *seagull* (or all seagulls) choosing to flap its (their) wings, in the context of an analysis of the finite-time predictability of incompressible vortical flows.] The process of projecting the initial data (vorticity components in the spectral domain) onto a finite-resolution physical grid of pressure and velocity components is an unavoidable source of small but widespread initial uncertainty, the effect of which is difficult to assess. Also, any calculation differences are likely to be greatest at early times when velocity gradients are very large and localized, and these early differences then have all the remaining time in which to grow and propagate to other scales. For this reason, the projection from spectral to physical domain was actually carried out when the centreplane mean velocity deficit had already decreased by about 15% (at time $\tau = 1.4$), but there may still have been a residual effect of high gradients from the plate. Probably the best that can be hoped for in a comparison is that simulations will continue to agree on flow statistics even though they will certainly diverge at the level of instantaneous details.

The results from the present work have shown that, within the limits of this type of comparison, there is remarkably little difference between results from AGE method DNS and from spectral DNS. The AGE method saves an order of magnitude in computational effort, however, and it is more flexible with regard to boundary conditions and can be used for spatially evolving simulations. Reducing the resolution by a factor of two or three (auto-LES) offers further gains in memory requirements and calculation time (a 92–98% reduction) without loss of information that would be valuable for engineering purposes, except perhaps where small scales are crucial such as combustion problems. It is postulated that AGE routines for controlling accuracy and numerical instability also have the effect of SGS stress, and that with further experience it will be possible to set the relevant parameter value as a function of grid Reynolds number. The next step is to determine whether the AGE method advantages can be maintained in wall-bounded flows, where many types of LES (including spectral) have not fared very well on coarse grids near the walls.

In general terms, the AGE method is an example of the idea that simple methods may play a very useful role in simulations of real turbulent flows, provided that they maintain reasonable accuracy and stability over a good range of Reynolds numbers. It is much easier to apply such methods in flows with complex boundary conditions. Similarly, there may be little benefit from developing complex and expensive models for LES, in certain flows at least, given that the present auto-LES results were obtained with no explicit model at all.

High-quality simulations of canonical flows, especially spectral DNS such as the planar wake [4] used here, will not become redundant, however. They will always be needed for comparison purposes and for investigations of the fundamentals of turbulent flow.

ACKNOWLEDGEMENTS

Dr Michael Rogers of the NASA Ames Research Center kindly made available the initial velocity fields and spectral results, and assisted through many helpful discussions. Both Dr Rogers and Dr Bendiks Boersma of the CTR reviewed a draft of this paper. Some of the calculations were carried out at the Australian National University Supercomputer Facility, which is gratefully acknowledged.

REFERENCES

1. Bisset DK. The AGE method for direct numerical simulation of turbulent shear flow. *International Journal for Numerical Methods in Fluids* 1998; **28**:1013–1031.
2. Bisset DK. Further development of the AGE method. In *Numerical Methods for Fluid Dynamics*, vol. VI, Baines MJ (ed.), Oxford University Computing Laboratory: Oxford, 1998; 245–251.
3. Lesieur M, Métais O. New trends in large-eddy simulations of turbulence. *Annual Review of Fluid Mechanics* 1996; **28**:45–82.
4. Moser RD, Rogers MM, Ewing DW. Self-similarity of time-evolving plane wakes. *Journal of Fluid Mechanics* 1998; **367**:255–289.
5. Spalart PR, Moser RD, Rogers MM. Spectral methods for the Navier–Stokes equations with one infinite and two periodic directions. *Journal of Computational Physics* 1991; **96**:297–324.
6. Ghosal S, Rogers MM. A numerical study of self-similarity in a turbulent plane wake using large-eddy simulation. *Physics of Fluids* 1997; **9**(6):1729–1739.
7. Weygandt JH, Mehta RD. Three-dimensional structure of straight and curved plane wakes. *Journal of Fluid Mechanics* 1995; **282**:279–311.
8. Bisset DK, Antonia RA. Three-dimensional simulations of turbulent planar jets. In *Advances in Turbulence*, vol. VII, Frisch U (ed.), Kluwer Academic Publishers: Dordrecht, 1998; 163–166.
9. Bisset DK. Numerical simulation of heat transfer in turbulent mixing layers. In *Proceedings of the 13th Australasian Fluid Mechanics Conference*, Thompson MC, Hourigan K (eds), Monash University, Clayton VIC, 1998; 21–24.
10. Bisset DK, Rogers MM. Comparison of AGE and spectral methods for the simulation of far-wakes. *Annual Research Briefs 1999*, Center for Turbulence Research, Stanford University, 2000; 423–430.
11. Spalart PR. Direct simulation of a turbulent boundary layer up to $Re_\theta = 1410$. *Journal of Fluid Mechanics* 1988; **187**:61–98.
12. Deardorff JW. A numerical study of three-dimensional turbulent channel flow at large Reynolds numbers. *Journal of Fluid Mechanics* 1970; **41**(2):453–480.
13. Ferziger JH. Large eddy simulation: an introduction and perspective. In *New Tools in Turbulence Modelling*, Métais O, Ferziger JH (eds), Springer: Berlin, 1997; 29–47.
14. Boris JP, Grinstein FF, Oran ES, Kolbe RL. New insights into large-eddy simulation. *Fluid Dynamics Research* 1992; **10**:199–228.
15. Garnier E, Mossi M, Sagaut P, Comte P, Deville M. On the use of shock-capturing schemes for large-eddy simulation. *Journal of Computational Physics* 1999; **153**(2):273–311.
16. Antonia RA, Bisset DK, Orlandi P, Pearson BR. Reynolds number dependence of the second-order turbulent pressure structure function. *Physics of Fluids* 1999; **11**(1):241–243.
17. Lorenz EN. The predictability of a flow which possesses many scales of motion. *Tellus* 1969; **21**(3):289–307.

